Eigenvalues of the Schrödinger equation with rational potentials

H. Scherrer, H. Risken, and T. Leiber
Abteilung für Theoretische Physik, Universität Ulm, D-7900 Ulm, Federal Republic of Germany
(Received 16 March 1988)

A matrix-continued-fraction algorithm which basically relies on an expansion of the eigenfunctions into complete sets is presented for calculating the eigenvalues of the one-dimensional Schrödinger equation with rational potentials. The method also applies to the corresponding three-dimensional central-force potentials. In particular, we investigate the one-dimensional nonpolynomial-oscillator potential $V_{\rm NPO}(x)=x^2+\lambda x^2/(1+gx^2)$, the eigenvalues of which are obtained for a large range of parameters λ and g. In the three-dimensional case we check the shifted $1/N$ expansion which has been applied to the nonpolynomial potential $V_{\rm NPO}(r)$ very recently. In addition to the numerical results, analytically exact solutions are given for a restricted class of such potentials. Moreover, we point out that the continued-fraction algorithm applies to a wider class of polynomial and nonpolynomial (rational) potentials. In summary, the matrix-continued-fraction algorithm is shown to produce the eigenvalues of essentially one-dimensional Schrödinger equations for a wide class of rational potentials with very high accuracy, and the proposed technique seems to offer several computational advantages compared to other numerical approaches applied in the field. Finally, an application of the continued-fraction algorithm to the two-variable Schrödinger equation is suggested.

I. INTRODUCTION

In quantum mechanics the calculation of the eigenvalues of the Schrödinger equation (SE) is a very important task. These eigenvalues can be obtained analytically for only few potentials, e.g., for the Coulomb potential, the Morse potential, the square-well potential, and the harmonic oscillator. Recently much effort has been given to generating (new) families of isospectral Hamiltonians[1] in order to extend the class of solvable quantum-mechanical potentials. Along this line of actual research, exact solutions were also found for the Hill equation and the Poeschl-Teller equation.[2] On the contrary, (one-dimensional) rational potentials, such as the nonpolynomial oscillator (NPO) $V_{\rm NPO}(x)=x^2+\lambda x^2/(1+gx^2)$, belong to a class of quantum-mechanical potentials which cannot be solved exactly in general. [The potential $V_{\rm NPO}(x)$ is of importance in nonlinear Lagrangian field theory and nonlinear optics[3] as well as in elementary particle physics.[4,5]] Nevertheless, a great deal of interest has been devoted to the investigation of the one-dimensional NPO $V_{\rm NPO}(x)$ in the last few years.[4–12] A wide spectrum of approaches, such as variational techniques,[7] the Padé approximant method,[9] the finite difference method,[6] perturbation schemes,[7,13] and expansions into complete sets,[11(b)] have been applied to the NPO. Only in a few cases has it been possible to obtain exact analytical solutions.[5,8,9] Very recently, the concept of supersymmetric quantum mechanics was applied to the NPO.[14] At present this property is also used in a variety of other fields of current interest.[15] However, all procedures mentioned above are somehow restricted. Most of the numerical methods which have been used up to now can only be applied to a limited range of the potential parameters, while the perturbation tools by definition are restricted to small deviations from the unperturbed problem. On the other hand, exact analytical solutions have only been found for a certain parameter dependence $\lambda=\lambda(g)$ and $\lambda\leq 0$.[5,8,9,14]

The three-dimensional NPO has recently been investigated[13] by means of the shifted $1/N$ method.[16] Particular emphasis was given to the study of the level splittings of certain energy levels which are degenerate in the limit $\lambda=0$ or $g=0$. For the following two reasons the accuracy of the computed energy eigenvalues and level splittings is an open problem:[13] On the one hand, no quantitative error bounds can be derived from the employed shifted $1/N$ expansion. There is only a rough estimate for the (λ,g) parameter domain where at least some of the calculated levels are no longer reliable, $\lambda^{1/2}/g\approx 3-30$; see Ref. 13. On the other hand, no eigenvalues for the three-dimensional NPO ($l\neq 0$) have been obtained by any other method. Therefore the calculation of these eigenvalues seems to be very important.

Another point of current interest is the eigenvalue problem of the SE with polynomial anharmonic potential which plays an important role in describing the dynamics of molecular vibrations. Such a type of problem has attracted the attention of many investigators over the years; see, e.g., Ref. 17. Recently a modified operator method (MOM) consisting of an appropriate partitioning of the Hamiltonian has been put forward by Fernández *et al.*[18] The MOM applies to symmetric as well as asymmetric potentials, provided the potential is a polynomial function of the coordinates.[18(a)] The same authors also obtained eigenvalues for a special type of parity-invariant anharmonic quantum-mechanical oscillators by means of the Rayleigh-Ritz variational method and expanding the eigenfunctions of the SE into a trigonometric basis set.[19] Very recently special interest has

been devoted by Fernández and Castro[20] to one-dimensional SE's with unsymmetric potentials. They used a generalization of the power-series method proposed by Killingbeck.[17]

In this paper a continued-fraction method is introduced for calculating the eigenvalues of the SE numerically. The algorithm is applicable to any effectively one- or two-dimensional potential which is represented by a rational (or polynomial) function and admits a discrete spectrum. For the one-dimensional SE with the nonpolynomial potential $V_{\mathrm{NPO}}(x)$ the eigenvalues are obtained by evaluating an ordinary continued fraction (OCF), while the three-dimensional case with the central-force potential $V_{\mathrm{NPO}}(r)$ and SE's with more complicated potentials are solved by means of matrix continued fractions (MCF).[21,22] We show that for a large range of potential parameters λ and g, the eigenvalues and eigenfunctions of the SE with the NPO can be calculated very effectively, i.e., the method is fast and leads to accurate results.

The outline of the paper is the following. In Sec. II we briefly summarize the basic features of the potential under study and its (physical) applications. In Sec. III the OCF algorithm is applied to the one-dimensional SE with the NPO potential $V_{\mathrm{NPO}}(x)$. Various eigenvalues of the one-dimensional NPO for a wide range of potential parameters and a detailed comparison with the results of other authors are also presented in this section. In Sec. IV we treat the three-dimensional SE with the central-force potential $V_{\mathrm{NPO}}(r)$. The usual expansion into spherical harmonics leads to an effectively one-dimensional SE. A comparison of our numerical results with recent perturbational calculations of Varshni[13] is also given. In Sec. V it is pointed out that a generalization of the MCF algorithm can be applied to solve the SE with a class of polynomial as well as nonpolynomial potentials. Finally, in Sec. VI we briefly summarize our results and propose an application of the MCF algorithm to effectively two-dimensional SE's.

II. MODEL AND ITS APPLICATIONS

We investigate the time-independent (one-dimensional) SE

$$\left[-\frac{d^2}{dx^2}+V_{\mathrm{NPO}}(x)\right]\Psi_n(x)=E_n\Psi_n(x)\ , \tag{2.1}$$

with the NPO potential

$$V_{\mathrm{NPO}}(x)=x^2+\lambda x^2/(1+gx^2),\quad g>0,\quad -\infty<x<\infty\ . \tag{2.2}$$

The SE (2.1) and the NPO potential (2.2) have been normalized in such a way that $\hbar^2/2m$ and the factor in front of x^2 in Eq. (2.2) are equal to 1. The NPO potential (2.2) occurs in several areas of physics, e.g., in laser theory,[3] in quantum field theory,[4,5] and in general relativity.[10(b)] Moreover, such a type of potential may also find application in macromolecular systems of biological origin.[23] The asymptotic behavior of the potential (2.2) for very large and very small x is evidently given by harmonic potentials; see Fig. 1.

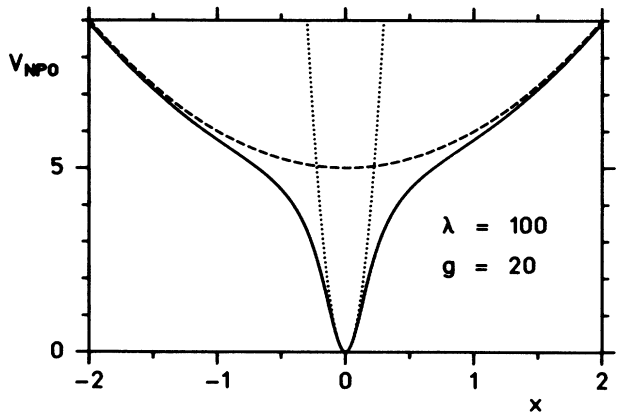

FIG. 1. Solid curve, nonpolynomial potential (2.2) with $\lambda=100$ and $g=20$; dotted and dashed curves, harmonic potentials describing the asymptotic behavior $x^2+\lambda/g$ (dashed line) and $(1+\lambda)x^2$ (dotted line).

In the three-dimensional case with the central-force potential $V_{\mathrm{NPO}}(r)$ the corresponding SE takes the form

$$[-\Delta+V_{\mathrm{NPO}}(r)]\hat{\Psi}_{n,l,m}(r,\theta,\phi)=E_{n,l,m}\hat{\Psi}_{n,l,m}(r,\theta,\phi)\ . \tag{2.3}$$

The usual expansion of the eigenfunction $\hat{\Psi}_{n,l,m}(r,\theta,\phi)$ into the radial part and spherical harmonics $Y_{l,m}(\theta,\phi)$, i.e.,

$$\hat{\Psi}_{n,l,m}(r,\theta,\phi)=(1/r)\Psi_{n,l}(r)Y_{l,m}(\theta,\phi)\ , \tag{2.4}$$

then leads to the one-dimensional SE

$$\left[-\frac{d^2}{dr^2}+V^l_{\mathrm{eff}}(r)\right]\Psi_{n,l}(r)=E_{n,l}\Psi_{n,l}(r)\ , \tag{2.5}$$

with the effective potential

$$V^l_{\mathrm{eff}}(r)=V_{\mathrm{NPO}}(r)+l(l+1)/r^2,\quad r\geq 0\ . \tag{2.6}$$

III. SOLUTION OF THE ONE-DIMENSIONAL SCHRÖDINGER EQUATION IN TERMS OF CONTINUED FRACTIONS

The solution of the eigenvalue problem of the one-dimensional SE by means of the OCF algorithm requires four steps. In the first step the eigenfunctions are expanded into an appropriate complete set. Next, we insert this expansion into the SE and obtain a tridiagonal recurrence relation for the expansion coefficients. In the third step this recurrence relation is solved by OCF's. (For the theory of continued fractions see, e.g., Ref. 24.) Finally, in the fourth step, the eigenvalues are obtained numerically by a root-finding technique.

A. Expansion of the eigenfunctions

As a complete set we use the eigenfunctions $|\nu\rangle$ of Eqs. (2.1) and (2.2) for $\lambda=0$, i.e., the harmonic-oscillator eigenfunctions which are defined through the relation

$$\mathbf{a}^\dagger\mathbf{a}\,|\,\nu\rangle=\nu\,|\,\nu\rangle\ , \tag{3.1}$$

where $\mathbf{a}^\dagger$ and $\mathbf{a}$ are the creation and annihilation operators

$$\mathbf{a}^\dagger=(x-d/dx)/\sqrt{2},\quad \mathbf{a}=(x+d/dx)/\sqrt{2}\ ,\qquad [\mathbf{a},\mathbf{a}^\dagger]=1\ . \tag{3.2}$$

The generally infinite expansion for $\lambda\neq 0$ then reads [see also Ref. 8(c)]

$$|\,\Psi_n\rangle=\sum_{\nu\geq 0}\bar{c}^{\,n}_\nu\,|\,\nu\rangle\ . \tag{3.3}$$

B. Tridiagonal recurrence relation

In order to obtain a recurrence relation for the expansion coefficients $\bar{c}^{\,n}_\nu$ we multiply the SE (2.1) with the denominator $1+gx^2$ of the NPO (2.2) and insert the expansion (3.3). Using

$$x=(\mathbf{a}+\mathbf{a}^\dagger)/\sqrt{2},\quad d/dx=(\mathbf{a}-\mathbf{a}^\dagger)/\sqrt{2}\ , \tag{3.4}$$

this equation then reads

$$\{(\mathbf{a}^2+\mathbf{a}^{\dagger 2})[g(2\mathbf{a}^\dagger\mathbf{a}+1-E_n)+\lambda]+g[4\mathbf{a}^\dagger\mathbf{a}(\mathbf{a}^\dagger\mathbf{a}+1)+1]+(2\mathbf{a}^\dagger\mathbf{a}+1)(\lambda+2-gE_n)-2E_n\}\sum_{\nu\geq 0}\bar{c}^{\,n}_\nu\,|\,\nu\rangle=0\ . \tag{3.5}$$

On employing the well-known relations

$$\mathbf{a}^\dagger\,|\,\nu\rangle=\sqrt{\nu+1}\,|\,\nu\rangle,\quad \mathbf{a}\,|\,\nu\rangle=\sqrt{\nu}\,|\,\nu-1\rangle\ , \tag{3.6}$$

Eq. (3.5) is easily evaluated. Reordering the expansion terms and making use of the completeness of the expansion set $|\,\nu\rangle$ immediately yields a tridiagonal recurrence relation for the expansion coefficients $\bar{c}^{\,n}_\nu$,

$$Q^-_\nu\bar{c}^{\,n}_{\nu-2}+Q_\nu\bar{c}^{\,n}_\nu+Q^+_\nu\bar{c}^{\,n}_{\nu+2}=0\ , \tag{3.7}$$

where the coefficients Q_ν and $Q^\pm_\nu$ are given by

$$\begin{aligned} Q^-_\nu&=\sqrt{\nu(\nu-1)}[g(2\nu-3-E_n)+\lambda]\ ,\\ Q_\nu&=(2\nu+1)[g(2\nu+1-E_n)+\lambda+2]-2E_n\ ,\\ Q^+_\nu&=\sqrt{(\nu+1)(\nu+2)}[g(2\nu+5-E_n)+\lambda]\ . \end{aligned} \tag{3.8}$$

The coupling of the coefficients $\bar{c}^{\,n}_\nu$ in Eq. (3.7) to nearest but one neighbors is an immediate consequence of the symmetry properties of the potential function (2.2) and the harmonic-oscillator eigenstates. Thus the determination of the eigenfunctions (and the corresponding eigenvalues) with even or odd parity are completely decoupled problems; see below.

C. Continued-fraction algorithm

On defining the transfer coefficients S_ν through the relation

$$\bar{c}^{\,n}_{\nu+2}=S_\nu\bar{c}^{\,n}_\nu\ , \tag{3.9}$$

the recurrence relation (3.7) reads ($\nu\geq 1$)

$$(Q^-_\nu/S_{\nu-2}+Q_\nu+Q^+_\nu S_\nu)\bar{c}^{\,n}_\nu=0\ . \tag{3.10}$$

In general the expansion coefficients $\bar{c}^{\,n}_\nu$ are different from zero. Therefore the transfer coefficients S_ν obey the two-term recurrence relation ($\nu\geq 0$)

$$S_\nu=-(Q_{\nu+2}+Q^+_{\nu+2}S_{\nu+2})^{-1}Q^-_{\nu+2}\ . \tag{3.11}$$

On repeatedly iterating Eq. (3.11) the S_ν can be expressed by OCF's,[21,22]

$$S_\nu=[-Q_{\nu+2}-Q^+_{\nu+2}[-Q_{\nu+4}-Q^+_{\nu+4}\cdots S_{\nu+N_{\max}}\cdots]^{-1}Q^-_{\nu+4}]^{-1}Q^-_{\nu+2}\ . \tag{3.12}$$

From the recurrence relation (3.7) we obtain for $\nu=k$, $k=0$, or $k=1$, depending on the parity of the eigenfunctions, even or odd, respectively,

$$(Q_k+Q^+_kS_k)\bar{c}^{\,n}_k=0,\quad k=0,1\ . \tag{3.13}$$

Here $S_k=S_k(E_n)$ is calculated by imposing the terminating condition $S_{N_{\max}}=0$, thus implying $\bar{c}^{\,n}_{N_{\max}+2}=0$ for the expansion coefficients. The convergence of the continued fraction S_k has to be ensured by a suitable choice of the terminating index $N_{\max}$, which represents the maximum oscillator eigenstate being considered [$N_{\max}$ is the upper bound of the truncated sum (3.3)]. Because the harmonic-oscillator eigenfunctions (3.1) form a complete set the expansion (3.3) should always work provided that the terminating index $N_{\max}$ is large enough. Approximate values for $N_{\max}$ may be obtained from the asymptotic solution of the recursion (3.7); for details see Ref. 11(a). In our numerical calculations $N_{\max}$ was determined in such a way that a further increase of $N_{\max}$ did not alter the final result within the prescribed accuracy (for further details see below).

D. Determination of eigenvalues

Depending on the parity of the eigenfunctions either all expansion coefficients $\bar{c}^{\,n}_\nu$ with odd ν are zero (even eigenfunction) or all $\bar{c}^{\,n}_\nu$ with even indices are zero (odd eigenfunctions). The first expansion coefficient $\bar{c}^{\,n}_0$ is generally different from zero for the even eigenfunctions, while for the odd eigenfunctions $\bar{c}^{\,n}_1$ is a nonvanishing quantity. Thus Eq. (3.13) leads to

$$D_k(g,\lambda,E_n)=Q_k+Q_k^+S_k(E_n)=0, \quad k=0,1 \qquad (3.14)$$

where $k=0,1$ is valid for even and odd eigenfunctions, respectively. From Eq. (3.14) the eigenvalues E_n are determined as the roots of $D_k=0$. By using some root-finding technique, the eigenvalues are thus obtained numerically.

E. Determination of eigenfunctions

The coefficients $\bar{c}_\nu^{\,n}$ with $\nu\geq 2$ can be easily computed by repeatedly employing Eq. (3.9); i.e.,

$$\bar{c}_\nu^{\,n}=S_{\nu-2}(E_n)S_{\nu-4}(E_n)\cdots S_k(E_n)\bar{c}_k^{\,n}, \quad k=0,1\ . \qquad (3.15)$$

By summing up the series (3.3) the (unnormalized) eigenfunction is thus obtained. It should be noted that the preceding procedure is numerically stable, whereas the repeated iteration of Eq. (3.10) starting with $\bar{c}_k^{\,n}$ and $\bar{c}_{k+2}^{\,n}=S_k\bar{c}_k^{\,n}$ $(k=0,1)$ is numerically unstable (see Chap 9 of Ref. 21).

F. Numerical results

In Fig. 2(a) the five lowest eigenvalues of the one-dimensional NPO (2.2) are displayed as a function of g for $\lambda=500$. Obviously the asymptotically harmonic behavior of the potential (2.2) for very small g values is reflected by the corresponding energy levels in Fig. 2(a). [Clearly, in the limit of very large g values the energy levels in Fig. 2(a) will also approach the corresponding harmonic-oscillator eigenvalues.] Of course, there exists an intermediate region of g values where the anharmonicity of the potential leads to a decrease of the eigenvalues with increasing g. A more detailed analysis of the level dynamics in that region is demonstrated in Fig. 2(b). The level spacings between two neighboring energy levels, $\Delta E=E_{2n}-E_{2n-1}$ $(n=1,2)$, corresponding to an even and an odd eigenfunction, respectively, exhibit (absolute) minima as a function of g. On the other hand, the spacing $\Delta E=E_{2n-1}-E_{2n-2}$ $(n=1,2)$ shows a relative maximum $(n=2)$ or is even a strictly monotonic function $(n=1)$.

In Table I we present a detailed comparison of the lowest eigenvalue of the one-dimensional NPO (2.2) with a variety of previously reported results. The most reliable results are those which have been calculated by Mitra[7(a)] and Hautot.[11(b)]

For the sake of completeness we give a brief account on the accuracy of our eigenvalues reported in Table I and Figs. 2. For demonstration we calculate the error of the ground-state energy E_0 of the one-dimensional NPO (2.2) for $\lambda=g=1$. If we choose $N_{\max}=20$ (120) the absolute error of the ground-state energy is 1×10^{-5} (3×10^{-13}), while for the precision requested in Table I (nine reliable digits) $N_{\max}=80$. It should be mentioned that for very large λ and/or g the necessary truncation index $N_{\max}$ increases considerably (up to several thousand). However, such a problem is easily circumvented by introducing an appropriate scaling of the expansion set; see, e.g., Sec. IV.

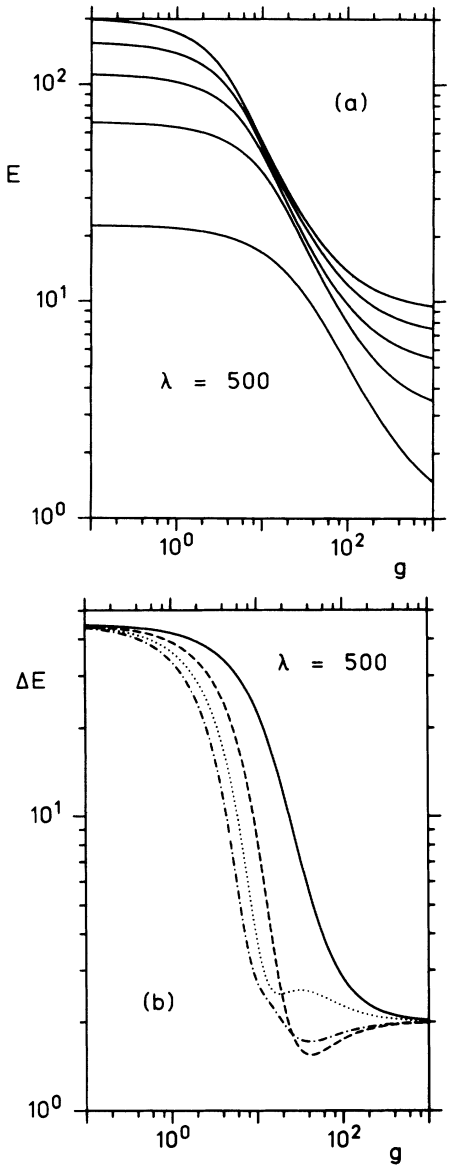

FIG. 2. One-dimensional NPO (2.1) and (2.2). (a) The five lowest eigenvalues E_n $(n=0$–$4)$ as a function of g for $\lambda=500$. (b) Level spacings as a function of g for $\lambda=500$: solid line, E_1-E_0; dashed line, E_2-E_1; dotted line, E_3-E_2; dotted-dashed line, E_4-E_3.

IV. SOLUTION OF THE THREE-DIMENSIONAL SCHRÖDINGER EQUATION IN TERMS OF MATRIX CONTINUED FRACTIONS

The three-dimensional SE (2.3) with the central-force potential $V_{\rm NPO}(r)$ reduces to a one-dimensional problem. Therefore we have to solve the one-dimensional eigenvalue equation (2.5) with the effective potential (2.6). The procedure is similar to the one-dimensional case discussed in Sec. III.

A. Expansion of the eigenfunction

We employ the rescaled expansion into the complete set of the Laguerre functions $\Phi_\nu^l(\alpha r)$,

TABLE I. Lowest eigenvalue of the one-dimensional NPO (2.1) and (2.2) for $\lambda, g = 1, 10, 100$.

		λ		
g	Results	1	10	100
1	MCF	1.232 350 72	2.782 330 52	9.359 418 03
1	Hautot[a]	1.232 35	2.782 33	9.359 42
1	Mitra[b]	1.232 35	2.782 33	9.3594
1	Bessis *et al.*[c]	1.232 372 05	2.782 330	9.359 418 03
1	Chaudhuri *et al.*[d]	1.242 13		
1	Lai *et al.*[e]	1.232 353 53	2.782 330 54	9.359 418 03
1	Kaushal[f]	1.227	2.754	9.3567
10	MCF	1.059 296 88	1.580 022 33	5.793 942 30
10	Hautot[a]	1.059 30	1.580 02	5.793 94
10	Mitra[b]	1.059 29	1.580 02	5.794
10	Bessis *et al.*[c]	1.059 297 00	1.580 024 9	5.793 947
100	MCF	1.008 410 60	1.084 063 34	1.836 335 83
100	Hautot[a]	1.008 41	1.084 06	1.836 34
100	Mitra[b]	1.008 41	1.084 06	1.8364
100	Bessis *et al.*[c]	1.008 410 6	1.084 064 3	1.836 385 0
100	Chaudhuri[d]		1.084 11	1.8411
100	Galacia *et al.*[g]			1.836 337 3

[a]Reference 11(b).
[b]Reference 7(a).
[c]Reference 7(b).
[d]Reference 10(a).
[e]Reference 9(b).
[f]Reference 9(a).
[g]Reference 6.

$$\Psi_{n,l}(\alpha r)=\sum_{\nu\geq 0}[\nu!\Gamma(\nu+l+\tfrac{3}{2})]^{1/2}c_\nu^{n,l}\Phi_\nu^l(\alpha r)\ ,$$
$$\Phi_\nu^l(r)=N_{\text{norm}}r^{l+1}\exp(-r^2/2)L_\nu^{l+1/2}(r^2)\ , \tag{4.1}$$

where L_ν^β denotes the generalized Laguerre polynomials[25] and N_{norm} is a suitable normalization constant. The scaling factor α allows for an improved convergence since through variation of α the expansion can be better adjusted to the exact eigenfunction. A systematic way for finding an appropriate scaling α has been presented in Ref. 11. It should be mentioned that the one-dimensional NPO (2.2) may be incorporated in the expansion (4.1) by setting $l=-1$ and $l=0$ for the eigenstates with even and odd parity, respectively. (However, the normalization of the expansion coefficients is different; see below.)

B. Tridiagonal vector recurrence relation

Inserting the expansion (4.1) into the eigenvalue equation (2.5) and using recurrence relations and differentiation formulas for the Laguerre polynomials,[25] we obtain, after some algebra, the pentadiagonal recurrence relation

$$Q_\nu^{2-}c_{\nu-2}^{n,l}+Q_\nu^{-}c_{\nu-1}^{n,l}+Q_\nu c_\nu^{n,l}+Q_\nu^{+}c_{\nu+1}^{n,l}+Q_\nu^{2+}c_{\nu+2}^{n,l}=0\ , \tag{4.2}$$

where the coefficients Q_ν, $Q_\nu^{\pm}$, and $Q_\nu^{2\pm}$ are given by

$$\begin{aligned}
Q_\nu^{2-}&=8(\alpha^4-1)g\ ,\\
Q_\nu^{-}&=8[(2g+\alpha^2)(1-\alpha^4)+\alpha^2\lambda\\
&\quad+g(4\nu+2l-1-\alpha^2E)]\ ,\\
Q_\nu&=g(1-\alpha^4)[4l(l+1)-3]\\
&\quad+4\alpha^2(4\nu+2l+3)(gE-\lambda-\alpha^4-1)\\
&\quad-g(4\nu+2l+3)^2(\alpha^4+3)+8\alpha^4E\ ,\\
Q_\nu^{+}&=8(\nu+1)(\nu+l+\tfrac{3}{2})[(2g-\alpha^2)(\alpha^4-1)+\alpha^2\lambda\\
&\quad+g(4\nu+2l+7-\alpha^2E)]\ ,\\
Q_\nu^{2+}&=8g(\alpha^4-1)(\nu+1)(\nu+2)(\nu+l+\tfrac{3}{2})(\nu+l+\tfrac{5}{2})\ .
\end{aligned} \tag{4.3}$$

With a scaling factor $\alpha=1$, the pentadiagonal recurrence relation (4.2) reduces to the tridiagonal recurrence relation (3.7) and the eigenvalue problem is solved by computing an OCF; see Sec. III. In that case the expansion (4.1) is related to Eq. (3.3) by setting

$$\tilde{c}_{2\nu+1+l}^{2n+1+l}=(-1)^\nu(\pi)^{1/4}[(2\nu+1+l)!/(2^{2\nu+l})]^{1/2}c_\nu^{n,l}\ ,\quad l=0,-1\ .$$

For $\alpha\neq 1$ the pentadiagonal recurrence relation (4.2) can be cast into a tridiagonal vector recurrence relation. On introducing the two-dimensional vectors

$$\mathbf{c}_\nu^{n,l}=\begin{bmatrix} c_{2\nu}^{n,l}\\ c_{2\nu+1}^{n,l}\end{bmatrix}\ , \tag{4.4}$$

Eq. (4.2) takes the form

$$\mathbf{Q}_\nu^- \mathbf{c}_{\nu-1}^{n,l} + \mathbf{Q}_\nu \mathbf{c}_\nu^{n,l} + \mathbf{Q}_\nu^+ \mathbf{c}_{\nu+1}^{n,l} = \mathbf{0}, \quad \mathbf{c}_{-1}^{n,l} = \mathbf{0} , \tag{4.5}$$

where the matrices $\mathbf{Q}_\nu$, and $\mathbf{Q}_\nu^\pm$ in Eq. (4.5) are given by

$$\mathbf{Q}_\nu^- = \begin{bmatrix} Q_{2\nu}^{2-} & Q_{2\nu}^- \\ 0 & Q_{2\nu+1}^{2-} \end{bmatrix} ,$$
$$\mathbf{Q}_\nu = \begin{bmatrix} Q_{2\nu} & Q_{2\nu}^+ \\ Q_{2\nu+1}^- & Q_{2\nu+1} \end{bmatrix} , \tag{4.6}$$
$$\mathbf{Q}_\nu^+ = \begin{bmatrix} Q_{2\nu}^{2+} & 0 \\ Q_{2\nu+1}^+ & Q_{2\nu+1}^{2+} \end{bmatrix} .$$

C. Matrix-continued-fraction algorithm

On defining the transfer matrices $\mathbf{S}_\nu$ through

$$\mathbf{c}_{\nu+1}^{n,l} = \mathbf{S}_\nu \mathbf{c}_\nu^{n,l} , \tag{4.7}$$

we obtain by insertion of Eq. (4.7) into the tridiagonal vector recursion (4.5) the matrix version of Eq. (3.11),

$$\mathbf{S}_\nu = -(\mathbf{Q}_{\nu+1} + \mathbf{Q}_{\nu+1}^+ \mathbf{S}_{\nu+1})^{-1} \mathbf{Q}_{\nu+1}^- . \tag{4.8}$$

Repeated iteration of Eq. (4.8) leads to the MCF for the transfer matrices $\mathbf{S}_\nu$. They are thus given by Eq. (3.12) after replacing the scalar quantities Q_k, $Q_k^\pm$, and S_k in Eq. (3.12) with the corresponding 2×2 matrices (4.6) and (4.8). [Note that the index (ν) notation in Eqs. (3.11) and (4.8) is different, since we have a nearest-neighbor coupling of the expansion vectors in Eq. (4.5), whereas $\bar{c}_\nu^{\,n}$ couples to $\bar{c}_{\nu\pm 2}^{\,n}$ in the one-dimensional case; see Eq. (3.7).]

D. Determination of eigenvalues

Insertion of Eq. (4.7) into Eq. (4.5) leads for $\nu=0$ to

$$(\mathbf{Q}_0 + \mathbf{Q}_0^+ \mathbf{S}_0)\mathbf{c}_0^{n,l} = \mathbf{0} , \tag{4.9}$$

where $\mathbf{S}_0$ is given by a MCF; see the matrix version of Eq. (3.12). The homogeneous system of Eqs. (4.9) admits to nontrivial solutions if and only if the determinant vanishes,

$$D(g,\lambda,E_{n,l},l) = \mathrm{Det}(\mathbf{Q}_0 + \mathbf{Q}_0^+ \mathbf{S}_0) = 0 . \tag{4.10}$$

The eigenvalues are again computed by some root-finding technique, while the eigenfunctions are obtained in close analogy to the OCF case; see Eq. (3.15).

E. Numerical results

The eigenvalues were calculated from Eq. (4.10) in double precision (16 digits). The results have been checked to be independent of the scaling parameter α. It should be mentioned, however, that different choices for the scaling parameter α require a new adjustment of the truncation index $N_{\max}$. In other words, an appropriate scaling of the expansion leads to a minimum number of iterations $N_{\max}$ necessary for achieving good convergence of the continued fraction (for more details, see, e.g., Ref. 11). Moreover, our algorithm has reproduced some exact analytical energy levels, e.g., $\lambda=-1040$, $g=10$, $n=0$, $l=1$, and $E_{0,1}=-95$ with an absolute error less than 10^{-12} setting $\alpha=1.6$ and using 12 matrix inversions. (Note that $\alpha\neq 1$ leads to a nonterminating MCF.) Numerical-integration methods similar to those employed in Ref. 6 and perturbational approaches have also been used (see the Appendix) and are in agreement with our numerical MCF results.

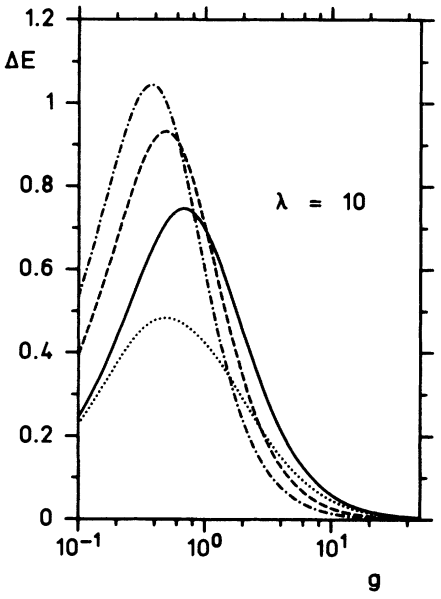

FIG. 3. Three-dimensional NPO (2.1) and (2.2). Level splitting $\Delta E = E_{n,l} - E_{n',l'}$ vs g for $\lambda=10$. Solid line, $E_{0,2}-E_{1,0}$; dashed line, $E_{0,3}-E_{1,1}$; dotted line $E_{1,2}-E_{2,0}$; dotted-dashed line, $E_{0,4}-E_{1,2}$.

In Figs. 3 and 4 we have plotted the same level spacings as in Figs. 2 and 3 of Ref. 13 (despite a factor of 0.5 which has been introduced in Ref. 13). We immediately

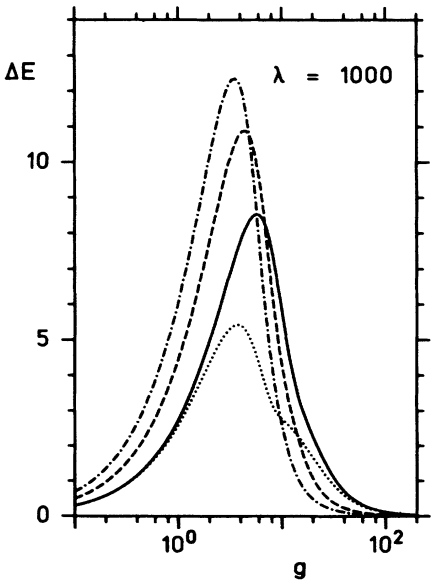

FIG. 4. Three-dimensional NPO (2.5) and (2.6). Level splitting ΔE vs g for $\lambda=1000$. Solid line, $E_{0,2}-E_{1,0}$; dashed line, $E_{0,3}-E_{1,1}$; dotted line $E_{1,2}-E_{2,0}$; dotted-dashed line, $E_{0,4}-E_{1,2}$.

recognize that curves D and B of Fig. 2 in Ref. 13 are almost identical, while the level splittings $\Delta E = E(1d) - E(2s)$ and, in particular, $\Delta E = E(2d) - E(3s)$ disagree completely. We conclude that the relative extrema of curves A and C for intermediate g values in Fig. 2 of Ref. 13 are an artifact of the perturbation method employed. Moreover, the results for large values of g in Ref. 13 also differ from our results, though the quantitative deviation is quite small. In general, the same arguments hold for the comparison of our Fig. 4 with Fig. 3 of Ref. 13. Substantial deviations are indicated by comparing curve C of Ref. 13 with our dotted line. Apart from the region $g \leq 1$ the actual shape of $\Delta E = E(2d) - E(3s)$ is quite different from that reported in Ref. 13; see, in particular, the positions of the extrema and the negative values in the region $g \approx 25-45$ in Ref. 13.

Figure 5 shows the same level splittings as reported above as a function of λ for $g = 10$. As demonstrated by our results the curves drawn in Fig. 5 of Ref. 13 are correct for $\lambda \leq 100$ but coincide only partially with our results for larger λ values. However, curve C in Ref. 13 disagrees with our results approximately by a factor of 2 over the whole λ range reported. Moreover, contrary to what was stated in Ref. 13, we confirm that the level

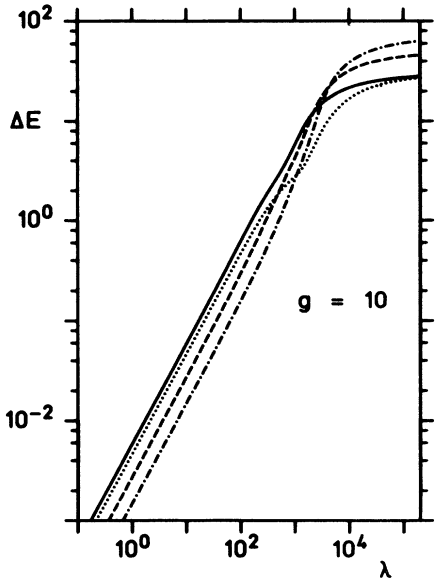

FIG. 5. Three-dimensional NPO (2.5) and (2.6). Level splitting ΔE vs λ for $g = 10$. Solid line, $E_{0,2} - E_{1,0}$; dashed line, $E_{0,3} - E_{1,1}$; dotted line $E_{1,2} - E_{2,0}$; dotted-dashed line, $E_{0,4} - E_{1,2}$.

TABLE II. Nine lowest eigenvalues of the three-dimensional NPO (2.5) and (2.6) (MCF results) for $\lambda = 10,100,1000$ and $g = 1,10,100,1000$. (Note that for comparison with Ref. 13 our results have to be multiplied with a factor 0.5.)

			g			
λ	n	l	1.00	10.00	100.00	1000.00
10.00	0	0	7.417 506	3.879 037	3.089 317	3.009 981
10.00	0	1	11.073 300	5.940 860	5.099 344	5.009 993
10.00	1	0	13.388 323	7.903 154	7.098 449	7.009 982
10.00	0	2	14.085 383	7.962 230	7.099 603	7.009 996
10.00	1	1	16.016 128	9.944 898	9.099 352	9.009 993
10.00	0	3	16.719 332	9.972 455	9.099 715	9.009 997
10.00	2	0	18.120 215	11.916 609	11.098 539	11.009 982
10.00	1	2	18.543 473	11.963 343	11.099 604	11.009 996
10.00	0	4	19.137 821	11.978 365	11.099 778	11.009 998
100.00	0	0	26.705 966	11.572 197	3.983 098	3.099 811
100.00	0	1	42.237 560	14.368 811	5.993 439	5.099 933
100.00	1	0	53.839 093	15.988 434	7.984 444	7.099 816
100.00	0	2	55.977 804	16.610 869	7.996 025	7.099 960
100.00	1	1	64.819 422	18.423 981	9.993 516	9.099 934
100.00	0	3	67.960 806	18.719 999	9.997 154	9.099 971
100.00	2	0	72.780 597	20.156 177	11.985 356	11.099 820
100.00	1	2	74.437 213	20.624 022	11.996 039	11.099 960
100.00	0	4	78.238 380	20.781 416	11.997 784	11.099 978
1000.0	0	0	91.256 611	64.825 083	12.823 345	3.998 107
1000.0	0	1	149.656 319	89.123 452	14.933 774	5.999 335
1000.0	1	0	203.363 285	94.875 967	16.839 571	7.998 158
1000.0	0	2	206.106 805	100.703 996	16.960 106	7.999 600
1000.0	1	1	256.161 362	101.225 824	18.934 595	9.999 335
1000.0	0	3	260.609 186	105.507 579	18.971 485	9.999 714
1000.0	2	0	304.521 713	103.184 601	20.850 027	11.998 195
1000.0	1	2	307.114 014	105.945 406	20.960 255	11.999 600
1000.0	0	4	313.164 667	108.527 834	20.977 814	11.999 778

splittings drawn in Fig. 5 (also) approach a constant value in the limit $\lambda \to \infty$. This asymptotic behavior may also be demonstrated by means of a perturbation approach; see the Appendix.

In Table II we depict the first nine energy levels of the three-dimensional NPO for different values of λ and g. In the parameter range which is not considered in our Table II but in Table II of Ref. 13 our results and those of Ref. 13 coincide (with only minor deviations on the last two decimal places). In Table II we focus on the "critical parameter region" $\lambda^{1/2}/g \approx 3-30$ as stated in Ref. 13. However, we find that even for smaller values $\lambda^{1/2}/g \approx 0.1-1$ the shifted $1/N$ expansion does not lead to accurate results. For $\lambda=10$ and $g=1$, for example, the $2p$ and $3s$ levels reported in Ref. 13 disagree with our results in all digits.

F. Analytical results for negative λ

For negative λ an application of the three-dimensional NPO to the shell model of the nucleus was also suggested in Ref. 13. According to the calculations carried out in Ref. 5 for the one-dimensional NPO (2.2), we make an ansatz for polynomial solutions of the form

$$\Psi_{n,l}(r)=P(r)r^{l+1}\exp(-r^2/2), \quad P(r)=\sum_{\nu=0}^{m} a_\nu r^{2\nu} . \tag{4.11}$$

Insertion of Eq. (4.11) into the SE (2.5) leads to a (finite) three-term recurrence relation for the coefficients a_ν,

$$\begin{aligned} &\alpha_\nu a_{\nu-1}+\beta_\nu a_\nu+\gamma_\nu a_{\nu+1}=0 , \\ &\alpha_\nu=g[E-\lambda/g+1-2(l+2\nu)] , \\ &\beta_\nu=E-3-2l-4\nu+2g\nu[2(l+\nu)+1] , \\ &\gamma_\nu=2(\nu+1)[2(l+\nu)+3] . \end{aligned} \tag{4.12}$$

It can be shown[5] that the nonzero roots λ of the determinant D_m of Eq. (4.12) are all negative. In other words, for fixed $g>0$ polynomial solutions of the type (4.11) exist only for $\lambda \le 0$. Terminating solutions (4.11) of Eq. (4.12) are obtained by requiring $a_\nu=0$ for $\nu \ge m+1$ (and $\nu<0$). Thus the eigenenergies are given by

$$E_{n,l}=4m+2l+3+\lambda/g , \tag{4.13}$$

while a certain algebraic relation between λ and g has to be a fulfilled, namely, $D_m=0$. As an example we calculate the ground-state energy $E_{0,l}$ (with $m=1$)

$$\begin{aligned} &E_{0,l}=2l+7+\lambda/g , \\ &\lambda=-4g-2g^2(2l+3) \quad (\text{or } \lambda=0) . \end{aligned} \tag{4.14}$$

Thus the $1p$ level for $\lambda=-0.5$ and $g=0.1$ is given by $E_{0,1}=4.0$, which supports the value reported in Table III of Ref. 13. [The trivial solutions $\lambda=0$ may be suppressed by splitting off a factor $(1+gr^2)$ from $P(r)$.]

V. APPLICATION OF THE CONTINUED-FRACTION ALGORITHM TO OTHER RATIONAL AND POLYNOMIAL POTENTIALS

The continued-fraction algorithms outlined in Secs. III and IV may also be applied to more complicated rational potentials. In the following, however, explicit expressions are restricted to one-dimensional problems. If, for instance, the potential has the form of a generalized parity-invariant rational function

$$V(x)=x^2+\left[\sum_{m=1}^{M}\lambda_{2m}x^{2m}\right]\Big/\left[1+\sum_{m=1}^{M}g_{2m}x^{2m}\right] , \tag{5.1}$$

the expansions (3.3) and (4.1) may be applied to the one-dimensional problem and to the three-dimensional central-force potential, respectively. [We assume that the coefficients g_{2m} of the potential (5.1) are chosen in such a way that the denominator never vanishes.] Multiplying the one-dimensional SE again with the denominator of the potential (5.1) and expressing x in terms of $\mathbf{a}$ and $\mathbf{a}^\dagger$ [see Eq. (3.4)], or repeatedly using the recurrence relation for the generalized Laguerre functions[25]

$$\begin{aligned} x^2L_\nu^\beta(x^2)=&-(\nu+1)L_{\nu+1}^\beta(x^2)+(2\nu+\beta+1)L_\nu^\beta(x^2) \\ &-(\nu+\beta)L_{\nu-1}^\beta(x^2) , \end{aligned} \tag{5.2}$$

we arrive at a recurrence relation of the form

$$Q_\nu^{-2M}c_{\nu-2M}^n+Q_\nu^{-2M+2}c_{\nu-2M+2}^n+\cdots+Q_\nu^{2M}c_{\nu+2M}^n=0 . \tag{5.3}$$

[For the three-dimensional SE with the central-force potential $V(r)$, Eq. (5.1), a similar expression is obtained. The only difference is again in the next-nearest-neighbor coupling of the expansion coefficients as already discussed for the NPO potential in Secs. III and IV.] Introducing the M-dimensional vector

$$\mathbf{c}_n^{n,l}=\begin{pmatrix} c_{2\nu}^{n,l} \\ c_{2\nu+2}^{n,l} \\ \vdots \\ c_{2\nu+2M}^{n,l} \end{pmatrix} , \tag{5.4}$$

the recurrence relation (5.3) can again be cast into a tridiagonal vector recurrence relation like Eq. (4.5), where the $M\times M$ matrices $\mathbf{Q}_\nu$ and $\mathbf{Q}_\nu^\pm$ follow from the coefficients $Q_\nu^{\pm 2m}$ $(m=0,1,2,\ldots,M)$ of Eq. (5.3). [Explicit expressions for transforming a recurrence relation with a finite coupling length into a tridiagonal vector recurrence relation can be found in Eqs. (9.17)–(9.19) of Ref. 21.]

Moreover, it should be mentioned that our generalized potential (5.1) also contains parity-invariant polynomial potentials for $g_{2m}=0$. If we choose $\lambda_{2m}=0$ for $m>2$, we simply obtain the quartic potential

$$V(x)=(1+\lambda_2)x^2+\lambda_4x^4, \quad \lambda_4>0 \tag{5.5}$$

which has been solved by means of 2×2 MCF's (Ref. 26) for $\lambda_2>-1$ (monostable potential) and also for $\lambda_2<-1$

(bistable potential). The recurrence relation corresponding to the monostable quartic potential (5.5) has already been given in Eq. (9.23) of Ref. 21. Thus it is demonstrated that the continued-fraction algorithm is also applicable to polynomial potentials. Of course, the application is not restricted to parity-invariant potentials. The one-dimensional SE with the unsymmetric potential

$$V(x)=x^2+\sum_{m=1}^{2M}\lambda_m x^m \Big/ \left[1+\sum_{m=1}^{2M} g_m x^m\right] \tag{5.6}$$

leads to a recurrence relation of the form

$$Q_\nu^{-2M}c_{\nu-2M}+Q_\nu^{-2M+1}c_{\nu-2M+1}+\cdots+Q_\nu^{2M}c_{\nu+2M}=0\ . \tag{5.7}$$

Here one has to introduce vectors of dimension $2M$,

$$\mathbf{c}_\nu=\begin{bmatrix} c_\nu \\ c_{\nu+1} \\ \vdots \\ c_{\nu+2M} \end{bmatrix}, \tag{5.8}$$

leading to $2M\times 2M$ MCF's. (We remark that the solution of the three-dimensional counterpart of the unsymmetric potential (5.6) requires some modifications of the employed expansion set, because the recurrence relations for the generalized Laguerre functions [see Eq. (5.2)] do not supply an expression for a term like $rL_\nu^\beta(r^2)$.)

For $\lambda_m=0$, $m\neq 3,4$, and $g_m=0$ the potential (5.6) reads

$$V(x)=x^2+\lambda_3 x^3+\lambda_4 x^4\ . \tag{5.9}$$

The anharmonic polynomial oscillator (5.9) has recently been investigated[18(b)] by means of an improved perturbational approach and eigenvalues of the SE have been calculated for small λ_3. We solved the SE with the potential (5.9), e.g., for $\lambda_3=0.2$ and $\lambda_4=0.01$. [Despite an overall factor of 0.5 in the SE this choice corresponds to $\alpha'=0.1$ and $\beta'=0.005$ in Ref. 18(b).] For these parameters, however, the potential (5.9) denotes a double-well potential. This bistable structure of the potential produces closely spaced pairs of energy levels provided that the potential barrier between the two wells is high enough.[27] That property of the eigenvalue spectrum has not been recognized in Ref. 18(b). Therefore the eigenvalues reported in Ref. 18(b) denote a sort of mean value of the two closely neighbored exact eigenvalues; see Table III. We remark that our eigenvalues reported in Table III are reliable in all digits. They have been checked by employing a 32-digit arithmetic and an increased truncation index $N_{\max}$. In order to achieve the required accuracy, $N_{\max}$ was chosen to be 15. Because the potential (5.9) represents a special case of the general potential form (5.6) with $M=2$, this problem leads to a 4×4 MCF. Therefore $N_{\max}=15$ corresponds to considering $4\times 15=60$ terms of the relevant expansion set. (Increasing $N_{\max}$ up to 400 and thus taking into account 1600 expansion terms leads to exactly the same results in all digits as reported in Table III.) However, we want to stress that the eigenvalues which have been presented in Ref. 18(b) for monostable anharmonic potentials (5.9) agree with our results, despite some deviations in the last four digits for the potential parameters $\alpha'=0.1$ and $\beta'=0.2$ ($\lambda_3=0.2$ and $\lambda_4=0.02$ in our units).

TABLE III. Ten lowest eigenvalues of the anharmonic polynomial oscillator (5.9) for $\lambda_3=0.2$ and $\lambda_4=0.01$.

	$E_{n/2}$ Results	
n	MCF	Fernández *et al.*[a]
0	0.489 497 520 976 06	0.489 497 827 01
1	0.489 498 132 721 21	
2	1.421 839 142 981 9	1.421 885 68
3	1.421 931 744 644 8	
4	2.265 520 000 152 4	2.268 171
5	2.270 646 160 254 7	
6	2.934 615 451 512 7	2.9792
7	3.030 663 815 953 6	
8	3.455 764 408 804 3	3.558
9	3.790 577 592 777 3	3.80

[a]Reference 18(b).

Very recently the concept of supersymmetric quantum mechanics was applied to the one-dimensional SE with the quartic double-well potential (5.5) for $\lambda_2<-1$ and $\lambda_4=1$.[28] The authors focused on calculating the tunneling rate in the limit of high potential barriers by a perturbational approach. For deep potential wells this tunneling rate is proportional to the energy difference of the lowest lying pair of eigenvalues.[27,28] In general, however, the smallness of the energy differences $\Delta E=E_1-E_0$ causes computational difficulties. This problem has been circumvented in Ref. 28 by regarding the supersymmetric partner potential. We have verified the tunneling rates reported in Ref. 28 by means of the MCF algorithm.

VI. CONCLUSIONS

It was our intention throughout the present investigation to demonstrate the power of the MCF algorithm for calculating the eigenvalues and eigenfunctions of the one-dimensional SE with arbitrary polynomial and non-polynomial potentials which admit a discrete spectrum. We have pointed out that our numerical results may be obtained over a wide range of potential parameters with high accuracy. This was demonstrated for the one-dimensional NPO $V_{\mathrm{NPO}}(x)$ and for its three-dimensional counterpart. In the latter case our results provide an accurate check on the shifted $1/N$ expansion which has been applied to the three-dimensional NPO very recently.[13] Moreover, we presented certain exact analytic solutions for the three-dimensional NPO. Our calculations for the three-dimensional NPO (see Figs. 3–5 and Table II) confirm that the perturbation approach employed in Ref. 13 does not lead to accurate results in the critical parameter range $\lambda^{1/2}/g\approx 0.1-30$.

A possible application of the MCF algorithm of SE's with more general rational potentials was also outlined. It was shown explicitly that the MCF method produces

reliable results for quartic (anharmonic) potentials. For bistable polynomial potentials (with high potential barriers) we have calculated the energy spectrum which consists of closely spaced pairs of energy levels. This enables us to confirm the tunneling rates which have been determined very recently in Ref. 28.

We also want to point out that in our opinion the proposed MCF algorithm for calculating eigenvalues of the time-independent SE is preferable to similar methods which have been suggested recently[29] because of its clear computational structure. The methods discussed, e.g., in Ref. 29 basically consist of solving the recurrence relation for the expansion coefficients directly. Another advantage of the MCF algorithm is that the precision of the calculated quantities may be easily checked and improved by increasing the relevant number of iterations $N_{\max}$. Since the computation time is proportional to $N_{\max}$ a considerable increase of $N_{\max}$ in general causes no computational problems.

Very recently, doubts have again been raised on the applicability of three-term recurrence relations to the eigenvalue problem of certain SE's.[30(a)] We would like to stress that the MCF algorithm does not suffer from these problems which led to some controversy in the recent literature on SE's with anharmonic polynomial potentials.[30] The expansion of the eigenfunctions of the SE into complete sets which have been employed herein should always guarantee the convergence of the MCF solution to the required solution of the SE. Finally, we state that from our experience discretization methods (see, e.g., Ref. 17) generally require more computation time than the MCF algorithm in order to achieve the same accuracy.

We conclude with suggesting the application of the MCF method to essentially two-dimensional SE's. For two-dimensional Fokker-Planck equations, eigenvalues and eigenfunctions have already been obtained by means of the MCF method.[21,31] In such a case one has to employ an expansion into two complete sets. Truncating one of these sets at $M_{\max}$, the dimension of the matrices to be inverted is of the order $M_{\max}$, while the other terminating index $N_{\max}$ still gives the number of iterations of the MCF. Therefore, compared with the one-dimensional case, the dimension of the matrices occurring in the MCF's increases considerably. Since two-dimensional Fokker-Planck equations are typically of the same structure as two-dimensional SE's, the method should also work for the SE with two variables. A nontrivial example, which is of importance in physics and chemistry, is the two-dimensional SE with the potential $V(x,y)=\omega_1^2x^2+\omega_2^2y^2+k_1x^4+k_2y^4-\lambda xy^2$. For such a potential of two nonlinearly coupled nonlinear oscillators an expansion into two sets of Hermite functions will lead to a recursion for the expansion coefficients with a finite coupling length and the MCF algorithm should therefore also be applicable.

ACKNOWLEDGMENTS

We wish to thank Professor Baltin and Professor Witschel for stimulating discussions. Two of us (H.R. and T.L.) gratefully appreciate financial support from the Deutsche Forschungsgemeinschaft.

APPENDIX: PERTURBATION THEORY FOR THE THREE-DIMENSIONAL NPO

A first-order perturbation theory is carried out for the three-dimensional NPO (2.5) and (2.6) in the limit $\lambda\to\infty$. Thus an analytic expression is given for the level splittings ΔE depicted in Fig. 5. The effective potential (2.6) reads

$$V_{\text{eff}}^{l}(r)=r^2+l(l+1)/r^2+\tilde{V}(r)\ , \tag{A1}$$

and we expand the denominator of $\tilde{V}(r)$,

$$\tilde{V}(r)=\lambda r^2/(1+gr^2)\approx\lambda r^2[1-gr^2+O(g^2r^4)]\ . \tag{A2}$$

The expansion in Eq. (A2) is valid for $r^2\ll 1/g$, a constraint which may be equally well replaced by $\langle r^2\rangle\ll 1/g$. Thus our approximated Hamiltonian operator is given by

$$\begin{aligned} H&=H^0+H^1\ ,\\ H^0&=-\frac{d^2}{dr^2}+l(l+1)/r^2+(\lambda+1)r^2\ ,\\ H^1&=-\lambda gr^4+O(\lambda g^2r^6)\ . \end{aligned} \tag{A3}$$

The solution of the unperturbed problem

$$H^0\Psi_{n,l}(r)=E_{n,l}\Psi_{n,l}(r) \tag{A4}$$

is given by

$$\begin{aligned} E_{n,l}&=(4n+2l+3)(1+\lambda)^{1/2}\ ,\\ \Psi_{n,l}&=N_{\text{norm}}r^{l+1}L_n^{l+1/2}(r^2(1+\lambda)^{1/2})\\ &\quad\times\exp[-r^2(1+\lambda)^{1/2}]\\ &\equiv(1+\lambda)^{1/8}\phi_{n,l}(r(1+\lambda)^{1/4})\ , \end{aligned} \tag{A5}$$

with the normalization constant N_{norm} and $\phi_{n,l}(r)$ denoting the solution of the SE in the case $\lambda=0$ (harmonic oscillator). Thus we obtain in first-order perturbation theory

$$\begin{aligned} \langle H^1\rangle&\approx\frac{-\lambda g}{1+\lambda}\langle\Psi_{n,l}(r)\,|\,r^4(1+\lambda)\,|\,\Psi_{nl}(r)\rangle\\ &=\frac{-\lambda g}{1+\lambda}\langle\phi_{n,l}(r)\,|\,r^4\,|\,\phi_{n,l}(r)\rangle\\ &=\frac{-\lambda g}{1+\lambda}[6n^2+3(2l+3)n+l^2+4l+\tfrac{15}{4}]\ . \end{aligned} \tag{A6}$$

[It can be shown that in the limit $\lambda\to\infty$ the infinite sum of the higher-order terms resulting from the expansion of the potential (A2) converges to zero.] The energy difference between two levels which are degenerate for $g=0$ is now calculated in the limit $\lambda\to\infty$,

$$\begin{aligned} &\lim_{\lambda\to\infty}\Delta E=g(n_1-n_2)[2(n_1-n_2+l_1)+1]\ ,\\ &\Delta E=E_{n_2,l_2}-E_{n_1,l_1},\quad l_2=2n_1-2n_2+l_1\ . \end{aligned} \tag{A7}$$

Thus we obtain for the level splittings reported in Fig. 5 in the limit $\lambda\to\infty$ $E_{0,2}-E_{1,0}=E_{1,2}-E_{2,0}=3g$, $E_{0,3}-E_{1,1}=5g$, and $E_{0,4}-E_{1,2}=7g$, in agreement with our numerical results in Fig. 5.

[1]P. B. Abrahams and H. E. Moses, Phys. Rev. A **22**, 1333 (1980); M. M. Nieto, Phys. Lett. **145B**, 208 (1984); B. Mielnik, J. Math. Phys. **25**, 3387 (1984); M. Luban and D. L. Pursey, Phys. Rev. D **33**, 431 (1986); D. L. Pursey, *ibid.* **33**, 1048 (1986); **33**, 2267 (1986); **36**, 1103 (1987).

[2]L. W. Casperson, Phys. Rev. A **30**, 2749 (1984); **31**, 2743(E) (1985); S.-M. Wu and C.-C. Shih, *ibid.* **A32**, 3736 (1985); A. B. Nassar and F. L. A. Machado, *ibid.* **35**, 3159 (1987).

[3]H. Risken and H. D. Vollmer, Z. Phys. **201**, 323 (1967); H. Haken, in *Laser Theory,* Vol. XXV/2c of *Encyclopedia of Physics* (Springer-Verlag, Berlin, 1970).

[4]S. N. Biswas, K. Datta, R. P. Saxena, P. K. Srivastava, and V. S. Varma, J. Math. Phys. **14**, 1190 (1973).

[5]R. R. Whitehead, A. Watt, G. P. Flessas, and M. A. Nagarajan, J. Phys. A **15**, 1217 (1982).

[6]S. Galicia and J. Killingbeck, Phys. Lett. **71A**, 17 (1979).

[7](a) A. K. Mitra, J. Math. Phys. **19**, 2018 (1978); (b) N. Bessis and G. Bessis, *ibid.* **21**, 278 (1980).

[8](a) G. P. Flessas, Phys. Lett. **83A**, 121 (1981); (b) V. S. Varma, J. Phys. A **14**, L489 (1981); (c) M. Znojil, *ibid.* **16**, 293 (1983).

[9](a) S. R. Kaushal, J. Phys. A **12**, L253 (1979); (b) C. S. Lai and H. E. Lin, *ibid.* **15**, 1495 (1982).

[10](a) R. N. Chaudhuri and B. Mukherjee, J. Phys. A **16**, 4031 (1983); (b) G. Marcilhacy and R. Pons, *ibid.* **18**, 2441 (1985); (c) C. R. Handy, *ibid.* **18**, 3593 (1985).

[11](a) A. Hautot and A. Magnus, J. Comput. Appl. Math. **5**, 3 (1979); (b) A. Hautot, J. Comput. Phys. **39**, 72 (1981).

[12]M. H. Blecher and P. G. L. Leach, J. Phys. A **20**, 5923 (1987).

[13]Y. P. Varshni, Phys. Rev. A **36**, 3009 (1987).

[14]R. Roy and R. Roychoudhury, Phys. Lett. A **122**, 275 (1987).

[15]M. Bernstein and L. S. Brown, Phys. Rev. Lett. **52**, 1933 (1984); V. A. Kostelecký and M. M. Nieto, *ibid.* **53**, 2285 (1984); T. D. Imbo and U. P. Sukhatme, *ibid.* **54**, 2184 (1985); P. Kumar, M. Ruiz-Altaba, and B. S. Thomas, *ibid.* **57**, 2749 (1986); R. Dutt, A. Khare, and Y. P. Varshni, Phys. Lett. A **123**, 375 (1987); for a review see, e.g., B. Freedman and F. Cooper, Physica **15D**, 138 (1985).

[16]T. Imbo, A. Pagnamento, and U. Sukhatme, Phys. Rev. D **29**, 1669 (1986); S. A. Maluendes, F. M. Fernández, and E. A. Castro, Phys. Lett. A **124**, 215 (1987).

[17]J. P. Killingbeck, Rep. Prog. Phys. **48**, 53 (1985), and references therein.

[18](a) F. M. Fernández, A. M. Mesón, and E. A. Castro, Phys. Lett. A **104**, 401 (1984); (b) Mol. Phys. **58**, 365 (1986).

[19]A. M. Méson, F. M. Fernández, and E. A. Castro, Z. Naturforsch. **38a**, 473 (1983).

[20]F. M. Fernández and E. A. Castro, Phys. Lett. A **124**, 1 (1987).

[21]H. Risken, *The Fokker-Planck Equation* (Springer-Verlag, Berlin, 1984).

[22]H. Scherrer, Diploma thesis, University of Ulm, 1987.

[23]W. Nadler and K. Schulten, J. Chem. Phys. **84**, 4015 (1986).

[24]O. Perron, *Die Lehre von den Kettenbrüchen* (Teubner, Stuttgart, 1977); Vols. I and II; H. S. Wall, *Analytic Theory of Continued Fractions* (Chelsea, New York, 1973); W. B. Jones and W. J. Thron, in *Continued Fractions,* Vol. 11 of *Encyclopedia of Mathematics and its Applications* (Addison-Wesley, Reading, MA, 1980).

[25]*Handbook of Mathematical Functions,* edited by M. Abramowitz and I. A. Stegun (Dover, New York, 1970).

[26]H. Denk, Ph.D. thesis, University of Ulm, 1984.

[27]L. D. Landau and E. M. Lifshitz, *Quantum Mechanics* (Pergamon, New York, 1977).

[28]W.-Y. Keung, E. Kovacs, and U. P. Sukhatme, Phys. Rev. Lett. **60**, 41 (1988).

[29]A. Hautot, Phys. Rev. D **33**, 437 (1986); F. M. Fernández, J. F. Ogilvie, and R. H. Tipping, J. Chem. Phys. **85**, 5850 (1986); D. A. Estrín, F. M. Fernández, and E. A. Castro, *ibid.* **87**, 7059 (1987).

[30](a) R. Roychoudhury and Y. P. Varshni, Phys. Rev. A **37**, 2309 (1988); (b) A. Hautot and M. Nicolas, J. Phys. A **16**, 2953 (1983); J. Killingbeck, *ibid.* **18**, L1025 (1985); R. N. Chaudhuri, Phys. Rev. D **31**, 2687 (1985); J. Killingbeck, J. Phys. A **20**, 1285 (1987); and references therein.

[31]H. D. Vollmer and H. Risken, Z. Phys. B **34**, 313 (1979); Physica **110A**, 106 (1982); K. Voigtlaender and H. Risken, J. Stat. Phys. **40**, 397 (1985); P. Jung and H. Risken, Z. Phys. B **61**, 367 (1985); T. Leiber, P. Jung, and H. Risken, *ibid.* **68**, 123 (1987); K. Vogel, H. Risken, W. Schleich, M. James, F. Moss, and P. V. E. McClintock, Phys. Rev. A **35**, 463 (1987); K. Vogel, T. Leiber, H. Risken, P. Hänggi, and W. Schleich, *ibid.* **35**, 4882 (1987); T. Leiber, F. Marchesoni, and H. Risken, Phys. Rev. Lett. **59**, 1381 (1987); T. Leiber, F. Marchesoni, and H. Risken, Phys. Rev. A **38**, 983 (1988); K. Vogel and H. Risken, *ibid.* **38**, 2409 (1988).